Radiationless Deactivation of an Intramolecular Charge Transfer Excited State through Hydrogen Bonding: Effect of Molecular Structure and Hard−Soft Anionic Character in the Excited State

Akimitsu Morimoito,[†] Tomoyuki Yatsuhashi,[†,‡] Tetsuya Shimada,[†] László Biczók,[§] Donald A. Tryk,[†,||] and Haruo Inoue*,[†,||]

Department of Applied Chemistry, Graduate Course of Engineering, Tokyo Metropolitan University, 1-1 Minamiohsawa, Hachiohji, Tokyo 192-0397, Japan, Chemical Research Center, Hungarian Academy of Science, P.O. Box 17, 1525 Budapest, Hungary, and CREST, Japan Science and Technology

Received: May 7, 2001; In Final Form: July 26, 2001

Energy-gap dependency for radiationless deactivation from excited states of various molecules having strong intramolecular charge transfer (ICT) character has been investigated by observing fluorescence quenching on addition of alcohols. Molecules having strong ICT excited states were classified into three groups: (a) molecules that underwent considerable fluorescence quenching by ethanol (quenching constant, $K_{SV} > 20\ M^{-1}$) and for which radiationless deactivation in protic solvents was much faster than anticipated from the ordinary energy-gap law observed in aprotic solvents, (b) molecules whose fluorescence exhibited substantial red shifts, and (c) molecules whose fluorescence were barely affected by the addition of ethanol ($K_{SV} < 1\ M^{-1}$) and for which the energy-gap dependences on radiationless deactivation in protic solvents were not so different from those in aprotic solvents. Typical fluorophores for each case, i.e., a, b, and c, were aminoanthraquinone, aminophthalimide, and aminocoumarin, respectively. Differences in the fluorescence quenching phenomena are discussed in terms of the molecular structure and the hard−soft anionic character of the excited states, governed by changes in charge density on the carbonyl oxygen. An excited molecule having a hard anionic character on a specific site within the molecule, classified as group a, was concluded to undergo considerable fluorescence quenching through an intermolecular hydrogen bonding interaction with an alcohol having a hard cationic character. On the other hand, fluorescence of an excited molecule having a soft anionic character, classified as group c, cannot be quenched well by an alcohol because of the weak interaction on the carbonyl oxygen. The anomalous behavior of the excited aminophthalimides (group b), which are classified as hard anions but do not undergo fluorescence quenching, suggested the possibility that molecular rigidity is another factor controlling the radiationless deactivation process induced by hydrogen bonding.

Introduction

The photophysical character of an excited molecule is greatly affected by polar solvent molecules such as alcohols.[1−17] Solvent molecules surrounding an excited molecule having strong intramolecular charge transfer (ICT) character have recently been revealed to exhibit not only a simple dielectrical relaxation behavior but also relaxation through specific types of solvation behavior. One of the typical types involves intermolecular hydrogen bonding of a protic solvent to an excited molecule.[7,9−17] Hydrogen bonding in the excited state has been one of the central subjects of studies in several laboratories, including ours.[5c−17] For the past decade, solvent dielectric relaxation of alcohols has attracted much attention and has been studied by theoretical simulation[3,4,9a] and ultrafast spectroscopy.[5b−7,9b,11] However, not so much attention has been paid to the specific solvation behavior that successively follows the dielectrical relaxation, because aminocoumarin derivatives themselves, which have been most often used for studies on dielectric relaxation, do not display much difference in fluorescence behavior for protic vs aprotic solvents.[8] On the other hand, we have recently found that alcohol molecules not only exhibit substantial specific solvation of the excited states of aminoanthraquinones (AAQ)[12] and aminofluorenones (AF)[13] but also induced efficient radiationless deactivation. The excited singlet states of AAQs and AFs deactivate very much faster in protic solvents than in aprotic ones. Specific solvation of a protic solvent such as an alcohol toward AAQ or AF induces an efficient radiationless deactivation through an intermolecular hydrogen bonding interaction between the hydroxyl group of the alcohol and the carbonyl groups of AAQ or AF. To gain an understanding of the details of the deactivation process mediated by specific solvation, it is most crucial to answer two questions: (1) why do alcohol molecules act as efficient quenchers and (2) what is the molecular mechanism? Detailed time-resolved fluorescence and transient absorption studies have revealed that the alcohol molecule interacts with the excited AAQs or AFs through two different types of intermolecular hydrogen bonds between the hydroxyl group of the alcohol and the carbonyl groups of AAQ or AF in (1) an in-plane mode

* To whom correspondence should be addressed. E-mail: inoue-haruo@c.metro-u.ac.jp.
[†] Tokyo Metropolitan University.
[‡] Present address: Department of Chemistry, Faculty of Science, Osaka City University, 3-3-138 Sugimoto, Sumiyoshi, Osaka 558-8585, Japan. E-mail: tomo@sci.osaka-cu.ac.jp.
[§] Hungarian Academy of Science.
[||] CREST (Japan Science and Technology).

10.1021/jp0117213 CCC: $20.00
Published on Web 10/16/2001

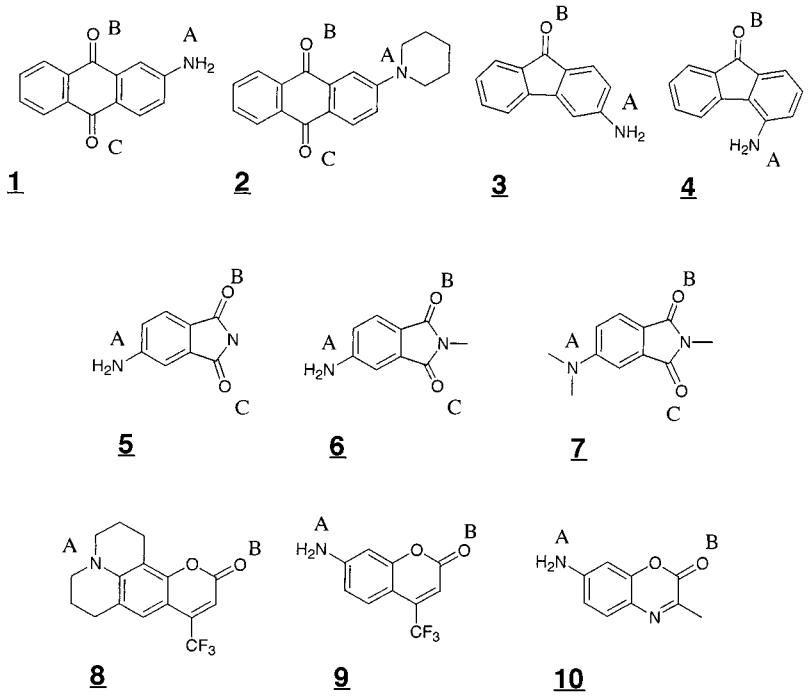

Figure 1. Molecules having an intramolecular charge-transfer excited state. The capital letters indicate electron-donating (A) and electron-accepting portions (B and C).

and (2) an out-of-plane mode with respect to the molecular plane of the aromatics.[14−17] The latter mode of interaction was presumed to be more important for the radiationless deactivation. Another promising approach to understand the molecular mechanism of the specific solvation and the radiationless deactivation would be to study what sorts of excited molecules are quenched by alcohols and to what extent.

In this paper, the fluorescence quenching behavior of 10 aromatic compounds having a strong ICT excited state was systematically investigated in order to understand in greater detail the molecular mechanism of specific solvation and radiationless deactivation through solvation modes such as intermolecular hydrogen bonding. The dependency of radiationless deactivation on the magnitude of the energy gap between the excited state and the ground state was examined in various solvents. The results obtained will be discussed in comparison with the degree of charge localization on specific sites within the molecule such as carbonyl oxygens.

Experimental Section

The structures of molecules used in this study are shown in Figure 1. 2-Amino-9,10-anthraquinone (**1**), 2-piperidino-9,10-anthraquinone (**2**), 3-amino-9-fluorenone (**3**), and 4-amino-9-fluorenone (**4**) were prepared as reported previously.[12,13] 4-Aminophthalimide (**5**; Tokyo Kasei) was purified by repeated recrystallization from ethanol/water mixture. 4-Amino-*N*-methylphthalimide (**6**; Tokyo Kasei) was purified by repeated recrystallization from a ethanol/benzene mixture. 4-*N*,*N*-Dimethylamino-*N*-methylphthalimide (**7**) was synthesized from **5** with treatment with methyl iodide and potassium hydroxide in dimethyl sulfoxide and was purified by column chromatography (silica gel, benzene/methanol) followed by recrystallization from a heptane/methanol mixture. Coumarin 153 (**8**; Aldrich) was used without further purification. Coumarin 151 (**9**; Aldrich) in CH_2Cl_2 was washed with 1 M aqueous NaOH, and the organic phase was dried over magnesium sulfate, evaporated, and further recrystallized from a methanol/water mixture. 7-Amino-3-methyl-1,4-benzoxazine-2-one (**10**) was synthesized[18] from 2, 5-diaminophenol and ethyl pyruvate in water then purified by column chromatography (silica gel, benzene/methanol) and recrystallization from ethanol. 2,5-Diaminophenol was prepared by the reduction of 2-amino-5-nitrophenol by sodium bisulfate. The purity of all materials were confirmed by NMR, MS, and TLC. All solvents were dried and purified before use.

The absorption spectra were recorded on a Shimadzu UV-2100PC spectrophotometer, and the corrected fluorescence spectra were measured with a Hitachi F-4010 spectrofluorometer. For measurement of fluorescence quantum yield, quinine bisulfate in 0.5 M aqueous sulfuric acid solution ($\Phi_f = 0.546$)[19] was used as the standard. Refractive index correction[20] was performed for each sample. The concentrations of the solutions prepared for estimation of fluorescence quantum yield were adjusted so as to be low enough to avoid inner filter effects. The fluorescence lifetimes were measured with a polychromator (CHROMEX 250IS)/streakscope (Hamamatsu, C4334) system. The samples were excited by an optical parametric generator (EKSPLA, PV-401, 420−560 nm, fwhm 25 ps, > 1 mJ/pulse) pumped by a Nd:YAG laser (EKSPLA, PL2143B, 25 ps fwhm, 15 mJ, 5 Hz) or by the third harmonic of a PL2143B under time-correlated single photon-counting conditions. The laser flux was adjusted by attenuation with neutral density filters to avoid multiphoton absorption processes and nonlinear effects. In these lifetime measurements, solvent relaxation process of aprotic solvents (within 10 ps)[5c] could not be observed because of the present time resolution (∼30 ps). Consequently, the decay profiles of all compounds in aprotic solvents could be fitted by single-exponential functions in all wavelength regions. In protic solvents, on the other hand, a relaxation process involving alcohols (with lifetimes of several tens of picoseconds) was observed.[5c,6] Therefore, the decay profiles were dependent on wavelength, and longer lifetimes obtained by double exponential fitting were defined as fluores-

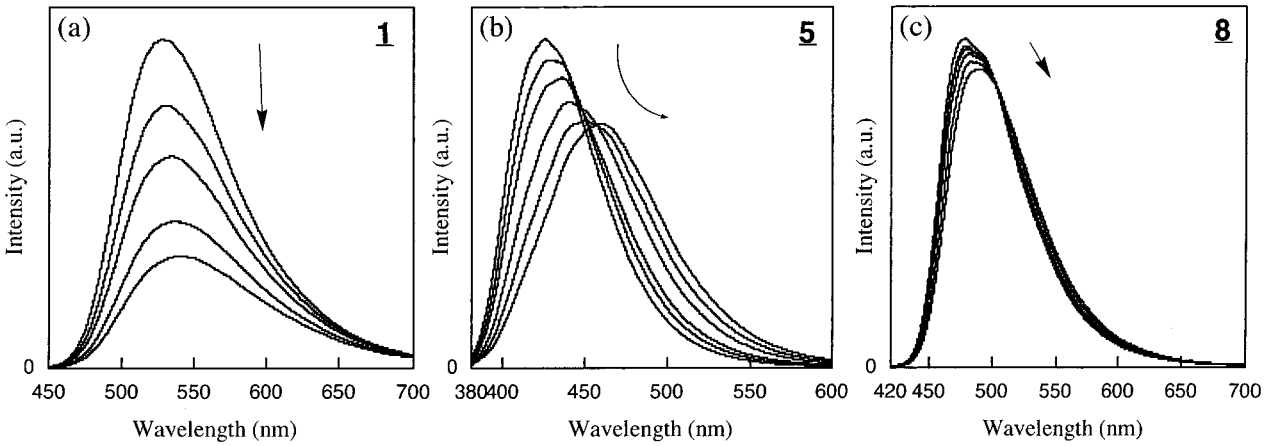

Figure 2. Fluorescence spectral changes of **1**, **5**, and **8** with the addition of ethanol in benzene. Ethanol concentrations are 0−0.06 (**1**), 0−0.06 (**5**), and 0−0.12 M (**8**), respectively. The direction of the arrow indicates increasing ethanol concentration.

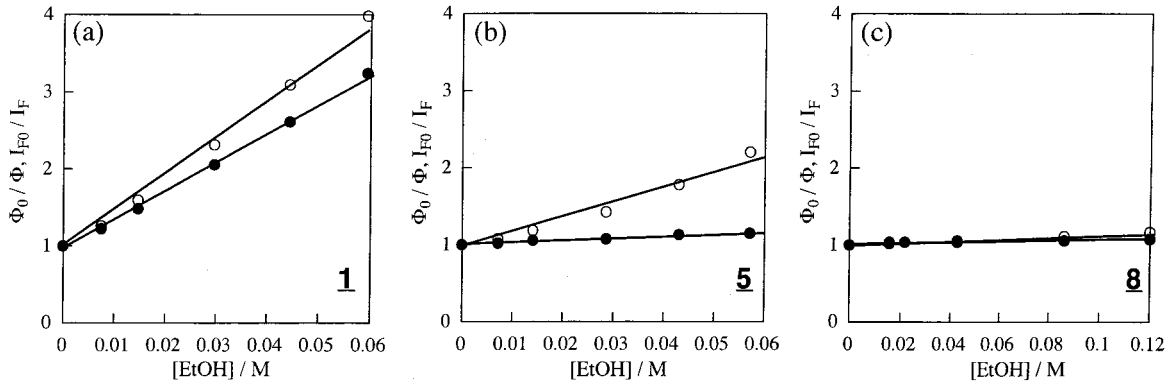

Figure 3. Stern−Volmer plots for fluorescence quenching for **1**, **5**, and **8** with ethanol, estimated by two types of analysis: (solid circles) plots obtained from the fluorescence quantum yield ratio; (open circles) plots obtained from the fluorescence intensity at the fluorescence maximum in benzene without ethanol (see text).

cence lifetime in protic solvents (see the Results and Discussion section also).

Nanosecond laser flash photolysis for measurement of triplet yield was carried out with a XeCl laser (308 nm, 12 ns fwhm) with a xenon lamp as a monitoring light source. The signal passing through the sample cell was detected by a photomultiplier tube (Hamamatsu Photonics R-666) at 490 nm. The energy transfer method was employed for estimation of triplet yield. Perylene was employed as a triplet energy acceptor, and 9-fluorenone was used as a standard. The detailed procedure has been described elsewhere.[21] All of the experiments were carried out at 297 K in ambient air. The partial charge calculations were carried out with the use of MOPAC 93 [PM3, C.I. = 4, full optimization in benzene (EPS = 2.274)] on an IBM RS/6000−590.

Results and Discussion

Fluorescence Quenching by Alcohols. The fluorescence behavior of various aromatic compounds, **1**−**10**, having strong ICT excited states in benzene upon addition of ethanol was examined. The absorption spectra of those aromatic compounds remained unchanged upon addition of ethanol in the concentration range examined (0−0.12 M). This suggests that the changes observed in the respective types of fluorescence behavior reflect dynamic aspects in the excited state caused by ethanol. Typical fluorescence spectral changes on addition of ethanol are shown in Figure 2. According to their characteristics, the compounds are classified into three groups. The compounds in the first group, represented by **1**, underwent drastic fluorescence quenching by ethanol (Figure 2a). The second group, represented by **5**, showed a substantial red shift of the fluorescence λ_{max} without appreciable quenching (Figure 2b). The fluorescence of the compounds in the third group was not affected at all by ethanol. A typical example is seen for **8** (Figure 2c). For discussing the degree of quenching, the fluorescence quenching efficiency was estimated by adopting the Stern−Volmer relation, indicated in eq 1:

$$\frac{\Phi_{F0}}{\Phi_F} = 1 + K_{SV}[\text{ethanol}] = 1 + k_q\tau_f[\text{ethanol}] \qquad (1)$$

where Φ_{F0}, Φ_F, K_{SV}, k_q, and τ_f denote the fluorescence quantum yields without and with ethanol, the Stern−Volmer constant, the fluorescence quenching rate constant, and the fluorescence lifetime in benzene, respectively. The Stern−Volmer plots for compounds **1**, **5**, and **8** are shown in Figure 3. The values obtained for K_{SV}, k_q, and τ_f are listed in Table 1. The fluorescence quenching estimated from the integral of the entire fluorescence band represents the total quenching efficiency of the excited state and involves the interaction with the alcohol and the relaxation of the solvent shell, as well as the emission efficiency from the relaxed state. Therefore, if the relaxed state, which is a hydrogen-bonded species in this case, is weakly emissive and supposing the fluorescence-quenching scheme is as that in Figure 4, the Stern−Volmer equation (eq 1) should be written in a more complicated form as shown in eq 2,

TABLE 1: Fluorescence Quenching by Ethanol in Benzene and Changes in Partial Charge for Particular Atoms with Photoexcitation

	K_{sv}[a]/M	τ[b]/ns	k_q[c]/10^9 M s^{-1}	E_{0-0}[d]/10^4 cm^{-1}	$\Delta\mu$[e]/D	partial charge changes[f] A	B	C
1	36.6 (48)	7.5	4.9	2.10	6.4	+0.38	−0.13	−0.08
2	31.4 (37)	9.5	3.3	1.88	7.1	+0.33	−0.13	−0.08
3	21.8 (29)	11	2.0	2.19	3.1	+0.21	−0.09	
4	24.7 (30)	9.2	2.7	2.03	5.0	+0.21	−0.09	
5	2.67 (19)	11	0.24	2.68	4.4	+0.32	−0.08	−0.04
6	1.90 (23)	14	0.14	2.53	4.6	+0.34	−0.09	−0.07
7	1.10 (4.1)	12	0.092	2.35	5.4	+0.29	−0.11	−0.08
8	0.58 (1.2)	4.1	0.14	2.22	5.8	+0.22	−0.03	
9	0.96 (2.8)	3.2	0.30	2.48	3.3	+0.26	−0.02	
10	0.63 (3.1)	2	0.19	2.54	5.2	+0.22	−0.02	

[a] Stern−Volmer constant (K_{SV}) was obtained for the fluorescence quantum yield. The value in the parentheses is obtained for fluorescence intensity at λ_{max} in benzene: 527 nm (**1**), 584 nm (**2**), 504 nm (**3**), 544 nm (**4**), 426 nm (**5**), 435 nm(**6**), 467 nm (**7**), 472 nm (**8**), 433 nm (**9**), 445 nm (**10**), respectively. [b] Fluorescence lifetime in benzene. [c] Quenching rate constant calculated by K_{SV}/τ. [d] The 0−0 transition energy in benzene determined by the normalized absorption and fluorescence spectrum. [e] Dipole moment change upon electronic excitation. [f] The partial charge changes of the particular atom A (nitrogen as a donor part), B, and C (oxygen as an acceptor part) indicated in Figure 1, from the ground state to the first excited singlet state calculated by MOPAC93 [PM3, C.I. = 4, full optimization in benzene (EPS = 2.274)]. A positive value means an increase in the charge density in the excited singlet state.

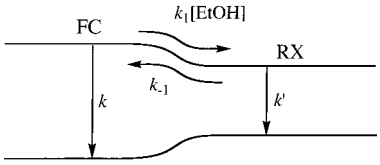

Figure 4. Two-excited-state diagram including the original fluorescent state (FC) and a single relaxed state (RX) involving hydrogen bonding. The rate constants k, k_1, k_{-1}, and k' denote the deactivation rate constant from FC to the ground state, the forward relaxation rate constant from FC to RX, the backward process from RX to FC, and the deactivation rate constant from RX to the ground state, respectively.

according to which the Stern−Volmer plots should show some curvature:

$$\frac{\Phi_{F0}}{\Phi_F} = \frac{1 + \dfrac{k_1 k'}{k(k_{-1} + k')}[\text{ethanol}]}{1 + \dfrac{k_f' k_1}{k_f(k_{-1} + k')}[\text{ethanol}]} \qquad (2)$$

where k, k_1, k_{-1}, and k' are the corresponding rate constants in Figure 4 and $k = k_f + k_{NR}$ and $k' = k_f' + k_{NR}'$ with k_f and k_f' being the radiative rate constants of the original fluorescence state and the relaxed state. k_{NR} and k_{NR}' denote radiationless deactivation rate constant of the original fluorescence state and the relaxed state, respectively. This kind of analysis had been reported for 3-aminofluorenone (**3**) in ref 15. For all of the compounds examined in this study, however, the deviation from a straight line is comparatively small. The apparent K_{SV} values estimated by use of eq 1 are listed in Table 1. On the other hand, in order to focus attention on the primary process, i.e., the interaction of ethanol with the excited state, another type of Stern−Volmer constant was estimated from the plot using *the relative fluorescence intensities at the fluorescence* λ_{max} with and without ethanol (I_{F0}/I_F). These types of Stern−Volmer plots

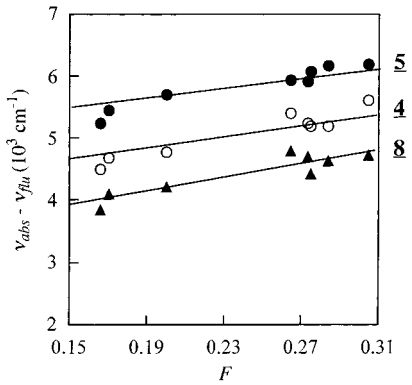

Figure 5. Lippert−Mataga plot for compounds **4**, **5**, and **8** in eight kinds of solvent (diethyl ether, butyl acetate, ethyl acetate, acetone, butyronitrile, acetonitrile, dimethyl formamide, and dimethyl sulfoxide).

are also shown in Figure 3, and the estimated K_{SV} values are given for comparison in parentheses in Table 1. Supposing that the initial interaction of the excited state with ethanol leads to complete quenching of the fluorescence, the two Stern−Volmer constants, one estimated from Φ_{F0}/Φ_F and the other from I_{F0}/I_F, should coincide with each other. The latter values, however, were generally larger than the former values. This difference was especially large for molecules **5** and **6**. These results indicate that in these compounds the emission intensity from the relaxed state is relatively high, even though the primary interaction with ethanol is efficient. On the other hand, for molecules **1**−**4**, the difference between the two K_{SV} values was small, indicating that the initial efficient interaction of ethanol leads to efficient quenching, without appreciable emission from the relaxed state. Compounds having a strong ICT excited state generally experience a large change in dipole moment in the excited state. The difference observed in the fluorescence behavior upon addition of ethanol, as shown in Figure 2 and Table 1 among the compounds examined here, may be ascribed to the degree of dipole moment change, which induces different degrees of dielectric interaction with ethanol. The dipole moment change between the excited and ground state was estimated by a Lippert−Mataga plot, based on eq 3.[22]

$$\nu_{abs} - \nu_{flu} = \frac{2(\Delta\mu)^2}{hca^3}F$$

$$F = \left[\frac{\epsilon - 1}{2\epsilon + 1} - \frac{n^2 - 1}{2n^2 + 1}\right] \qquad (3)$$

where $\nu_{abs} - \nu_{flu}$, a, ϵ, and n denote the wavenumber difference between the absorption and fluorescence maxima, the cavity radius in Onsager's theory of reaction field, the dielectric constant of the surrounding solvent medium, and the refractive index, respectively. The cavity radius a employed in eq 3 was estimated from a molecular volume calculation (ARVOMOL, version 2) [23] under the assumption that the molecular shape can be approximated as a sphere. The results are shown in Figure 5. The estimated dipole moment changes ($\Delta\mu$) are listed in Table 1. All compounds showed relatively large increments in the dipole moment in the excited state, indicating that the excited states for all have strong ICT character. The relaxational behavior of polar solvent molecules is generally known to be governed by a sudden change in dipole moment of the solute molecule.[5,6] Very interestingly, however, compounds **4** and **8** have quite different fluorescence quenching rate constants (k_q), even though the dipole moment changes are almost the same.

This clearly indicates that the overall dipole moment change in the excited state is not directly correlated to the radiationless deactivation induced by ethanol. It also suggests that the molecular mechanism of solvent relaxation followed by the radiationless process should be strongly dependent on the molecular structure and the more microscopic electronic structural differences in the excited state. Because the radiationless deactivation induced by ethanol is considered to be caused by intermolecular hydrogen bonding interactions,[12−17] the more microscopic factors that could affect the hydrogen bonding should be taken into account in order to understand the results.

We have already reported that the intermolecular hydrogen bond between the carbonyl groups of compounds **1**−**4** and the hydroxyl group of the alcohol acts as an accepting mode for the radiationless transition.[12,13] The contrasting differences in the ethanol-induced fluorescence quenching behavior shown in Table 1 promise to provide clues to the molecular mechanism of the efficient radiationless deactivation.

Effect of Energy Gap on the Radiationless Deactivation. As described above, the overall fluorescence quenching Stern−Volmer constant in benzene, estimated from Φ_{F0}/Φ_F upon addition of ethanol, contains both the efficiency of the primary interaction of ethanol with the excited state and the efficiency of deactivation from the relaxed state. To discuss solely the deactivation process, the rate constant of radiationless deactivation was measured in various solvents. The rate constant of radiationless transition to the ground state is generally known to depend on the energy gap between the excited and ground states, as indicated by the following equation:[24]

$$k_{IC} = \frac{C^2(2\pi)^{1/2}}{h(\Delta E h\omega_M)^{1/2}} \exp\left(-\frac{\gamma \Delta E}{h\omega_M}\right) \quad (4)$$

where ΔE, C, h, ω_M and γ denote the energy gap between the excited and ground states, the electronic coupling matrix element, the Planck constant, the wavenumber of the accepting vibrational mode of the radiationless transition, and a constant, respectively. Recently, Biczók et al. have reported that the internal conversion from the excited state of 2-substituted fluorenones and of various aminofluorenones showed beautiful energy-gap dependency.[25] Steer et al. have also found a similar relation in the internal conversion from S_2 of azulenes to their ground state.[26] In the present work, we have examined the relation between the energy gap of S_0-S_1 and the radiationless deactivation for the 10 compounds **1**−**10**, which all have strong ICT excited states in various protic solvents (methanol, ethanol, 1-propanol, 2-propanol, 1-butanol, *tert*-butyl alcohol, 1-octanol, and ethylene glycol) and aprotic solvents (dimethyl sulfoxide (DMSO), dimethyl formamide (DMF), acetonitrile, butyronitrile, ethyl acetate, benzene, and diethyl ether). All of the compounds studied (**1**−**10**) contain carbonyl groups. The rate constant for radiationless deactivation, k_{NR}, is expressed as the sum of those for internal conversion (k_{IC}) and intersystem crossing (k_{ISC}):

$$k_{NR} = k_{IC} + k_{ISC} \quad (5)$$

Among the compounds examined in this study, very small contributions from intersystem crossing have been reported for aminofluorenones[27] and aminocoumarins.[28] Furthermore, triplet yield (Φ_{ISC}) values for aminoanthraquinones and aminophthalimides estimated by nanosecond laser flash photolysis were rather low (Φ_{ISC} values for **1**, **2**, and **5**−**8** in acetonitrile and ethanol were less than 0.09). These results suggest that the radiationless deactivation rate constant (k_{NR}) estimated from eq 6 corresponds essentially to internal conversion (k_{IC}):

$$k_{NR} = (1 - \Phi_F)/\tau_f \cong k_{IC} \quad (6)$$

The energy gap, ΔE [$E(S_0) - E(S_1)$], was determined from the crossing point of the normalized absorption and fluorescence spectra. Photophysical properties of compounds **3**, **6**, and **8** are shown in Tables 2−4. Fluorescence decay profiles for all compounds in all aprotic solvents were well fitted by a single-exponential function. This indicates that observed profiles reflect the intrinsic deactivation process of the excited fluorophores after completion of the relaxation of the solvent molecules. On the other hand, decay profiles of all compounds in protic solvents were dependent on wavelength and could be fitted by double exponential functions. As a typical example, the time-resolved fluorescence profiles of 3-aminofluorenone in 2-propanol are

TABLE 2: Photophysical Properties of the 3-Aminofluorenone (3) in Protic and Aprotic Solvents[a]

solvent	Φ_f	τ_f (ns)	E_{0-0} (10^4 cm^{-1})	k_f[c] (10^7 s^{-1})	k_{NR}[c] (10^8 s^{-1})
ethylene glycol	0.0020	0.20[b]	1.94	1.0	51
methanol	0.0020	0.22[b]	1.94	0.91	45
ethanol	0.0033	0.29[b]	1.97	1.1	34
1-propanol	0.0037	0.32[b]	1.95	1.1	31
2-propanol	0.0050	0.41[b]	1.98	1.2	24
1-butanol	0.0042	0.34[b]	1.96	1.2	29
tert-butanol	0.0083	0.62[b]	2.00	1.3	16
1-octanol	0.0089	0.75[b]	2.01	1.2	13
DMSO	0.036	2.4	2.02	1.5	4.0
DMF	0.048	3.2	2.04	1.5	3.0
acetonitrile	0.043	5.9	2.08	0.73	1.6
butyronitrile	0.075	5.1	2.10	1.5	1.8
ethyl acetate	0.10	6.6	2.14	1.5	1.4
diethyl ether	0.14	8.0	2.18	1.8	1.1
benzene	0.13	11	2.19	1.2	0.79

[a] Φ_f, τ_f, E_{0-0}, k_f, and k_{NR} are fluorescence quantum yield, fluorescence lifetime, 0−0 transition energy of excited singlet state, radiative rate constant, and radiationless deactivation rate constant, respectively. [b] The fluorescence decay was fitted by a double exponential function, and a longer time component was employed as the lifetime. [c] Calculated with Φ_f and τ_f.

TABLE 3: Photophysical Properties of the 4-Amino-*N*-methylphthalimide (6) in Protic and Aprotic Solvents[a]

solvent	Φ_f	τ_f (ns)	E_{0-0} (10^4 cm^{-1})	k_f[c] (10^7 s^{-1})	k_{NR}[c] (10^8 s^{-1})
ethylene glycol	0.061	3.3[b]	2.20	1.8	2.8
methanol	0.10	5.3[b]	2.21	1.9	1.7
ethanol	0.19	8.2[b]	2.21	2.3	0.99
1-propanol	0.18	8.5[b]	2.20	2.1	0.96
2-propanol	0.25	9.5[b]	2.21	2.6	0.79
1-butanol	0.22	8.3[b]	2.21	2.6	0.94
tert-butanol	0.43	12[b]	2.21	3.7	0.49
1-octanol	0.32	9.6[b]	2.22	3.4	0.71
DMSO	0.64	16	2.27	4.5	0.25
DMF	0.56	14	2.31	4.6	0.35
acetonitrile	0.55	15	2.38	3.6	0.29
butyronitrile	0.50	13	2.40	4.5	0.45
ethyl acetate	0.49	11	2.44	4.8	0.51
diethyl ether	0.50	13	2.48	4.7	0.48
benzene	0.71	14	2.53	5.2	0.21

[a] Φ_f, τ_f, E_{0-0}, k_f, and k_{NR} are fluorescence quantum yield, fluorescence lifetime, 0−0 transition energy of excited singlet state, radiative rate constant, and radiationless deactivation rate constant, respectively. [b] The fluorescence decay was fitted by double exponential function, and a longer time component was employed as the lifetime. [c] Calculated with Φ_f and τ_f.

TABLE 4: Photophysical Properties of the Coumarin 153 (8) in Protic and Aprotic Solvents[a]

solvent	Φ_f	τ_f (ns)	E_{0-0} (10^4 cm^{-1})	k_f[c] (10^7 s^{-1})	k_{NR}[c] (10^8 s^{-1})
ethylene glycol	0.20	3.0[b]	2.02	6.8	2.7
methanol	0.32	3.7[b]	2.07	8.6	1.8
ethanol	0.40	4.5[b]	2.09	8.9	1.3
1-propanol	0.46	4.2[b]	2.09	11	1.3
2-propanol	0.51	4.5[b]	2.11	11	1.1
1-butanol	0.48	4.4[b]	2.10	11	1.2
tert-butanol	0.61	4.8[b]	2.13	13	0.82
1-octanol	0.56	4.7[b]	2.12	12	0.94
DMSO	0.46	4.1	2.08	11	1.3
DMF	0.51	4.3	2.09	12	1.1
acetonitrile	0.51	5.4	2.12	9.4	0.91
butyronitrile	0.57	4.4	2.13	13	0.98
ethyl acetate	0.63	4.0	2.19	16	0.93
diethyl ether	0.76	3.9	2.26	19	0.62
benzene	0.72	4.1	2.23	18	0.68

[a] Φ_f, τ_f, E_{0-0}, k_f, and k_{NR} are fluorescence quantum yield, fluorescence lifetime, 0−0 transition energy of excited singlet state, radiative rate constant, and radiationless deactivation rate constant, respectively. [b] The fluorescence decay was fitted by double exponential function, and a longer time component was employed as the lifetime. [c] Calculated with Φ_f and τ_f.

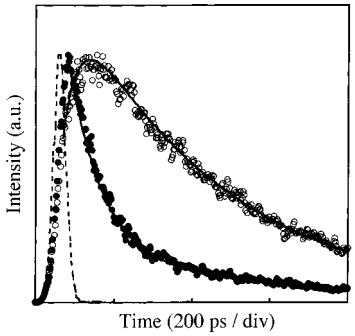

Figure 6. Fluorescence decay profile of 3-aminofluorenone (**3**) in 2-propanol: (solid circles) 515−530 nm; (open circles) 625−640 nm. The curves show the fittings to a double exponential decay with time constants of 50 and 410 ps. The dotted curve shows the laser pulse (355 nm).

shown in Figure 6. The fluorescence decays at the two different wavelengths were well fitted with two time constants, 50 and 410 ps, as shown in Figure 6. This kind of behavior was observed for all compounds in all protic solvents examined in this study. The short-time components (20 ∼ 80 ps) are in good agreement with the slowest relaxation process by alcohol solvents[5c,6]. Therefore, the longer-time components obtained by double-exponential fitting were designated as the fluorescence lifetimes in the protic solvents. Typical plots of the radiationless deactivation rate constants estimated by use of eq 6 as a function of ΔE for compounds **1**−**10** are shown in Figure 7. These have been classified into three groups according to their characteristics. The groupings turned out to be the same as those based on the fluorescence spectral behavior shown in Figure 2a−c. The first group contains compounds **1**−**4**, for which only the radiationless deactivation in protic solvents deviates enormously from the linear energy gap relation in aprotic solvents (curve 1 in Figure 7); the radiationless deactivation only in protic solvents was by far enhanced (Figure 7a). Also, compounds **5**−**7** form a second group for which the energy gap dependency exhibited different linear relationships for protic vs aprotic solvents; the slope for protic solvents (curve 2 in Figure 7) was steeper than that for aprotic ones (curve 1 in Figure 7). These results strongly suggest that the radiationless deactivation for the first and second groups in protic solvents follows a different molecular mechanism from that in aprotic solvents. On the other hand, although the third group, aminocoumarins **8**−**10**, exhibited different linear relationships between protic and aprotic solvents, the slope difference was significantly smaller as compared with other groups, e.g., aminoanthraquinones and aminophthalimides. This suggests that the radiationless deactivation of the third group of compounds has a similar molecular mechanism, irrespective of the nature of the solvent. Therefore, intermolecular hydrogen bonding does not contribute significantly to the deactivation, even though compounds **8**−**10** have strong ICT excited states and both amino and carbonyl groups within the molecule, just as the compounds in the first and second group do. It should also be noted here that the data in DMSO and DMF are well fitted by the linear curve for aprotic solvents (curve 1 in Figure 7) for all of the compounds **1**−**10**. Because DMSO and DMF are hydrogen bond-accepting solvents, these results coincide well with the previous consideration that the amino hydrogens of aromatic compounds such as **1**, **3**, and **4** do not contribute anything to the intermolecular hydrogen bond that causes the efficient deactivation.[12,13]

In Table 5, values for the degree of deviation of the deactivation rate constant in ethanol and methanol obtained as the value extrapolated from the energy gap relation (curve 1 in Figure 7) observed in aprotic solvents are summarized as $\Delta \ln k_{nr}$ {= $\ln k_{nr}$ (experimental value) − $\ln k_{nr}$ (value extrapolated from curve 1 in Figure 7)}. The values of $\Delta \ln k_{nr}$ were much larger for AAQs and AFs (**1**−**4**) than for the aminophthalimides (**5**−**7**), indicating that the intermolecular hydrogen bonding that is responsible for deactivation is more effective for compounds **1**−**4** than for compounds **5**−**7**. The rate constants for radiationless deactivation are also correlated well with the Taft donating hydrogen-bond parameter for alcohols,[29] supporting the consideration that the degree of hydrogen bonding with the alcohol hydroxyl group directly affects the radiationless deactivation (Figure 8).

Hard−Soft Anionic Character of the Excited States. Why do AAQs and AFs behave differently from other aromatic compounds? Why are the excited states of AAQs and AFs quenched so efficiently by alcohols? These are two key questions for the present study. As described above, all of the compounds examined here have strong ICT excited states and both amino and carbonyl groups within the molecules. The simple dielectric relaxational behavior of alcohols is not the only explanation for the efficient deactivation observed for **1**−**4**. More microscopic factors should be responsible for the efficient deactivation. A probable answer to the question would involve the local charge density on the carbonyl oxygen within the molecule. In Table 1, the partial changes in charge density upon excitation to the ICT excited state at specific sites such as the amino nitrogen as a donor site and the carbonyl oxygen as an acceptor site are compared. These values were estimated by means of PM3 MO calculations. The charge distributions in the excited states are also depicted schematically in Figure 9. In all of the compounds, the local charge densities on the amino nitrogen clearly decreased, indicating that all of the compounds (**1**−**10**) have substantial ICT from the amino groups within the molecules in the excited states. Very interestingly, on the other hand, the transferred negative charge was mostly localized on the carbonyl oxygen in the case of compounds **1**−**7**, whereas compounds **8**−**10** show substantial delocalization of the negative charge over the whole molecule (Figure 9). These contrasts in the negative charge distribution can be well discussed by a concept similar to HSAB (hard−soft acid−base theory).[30]

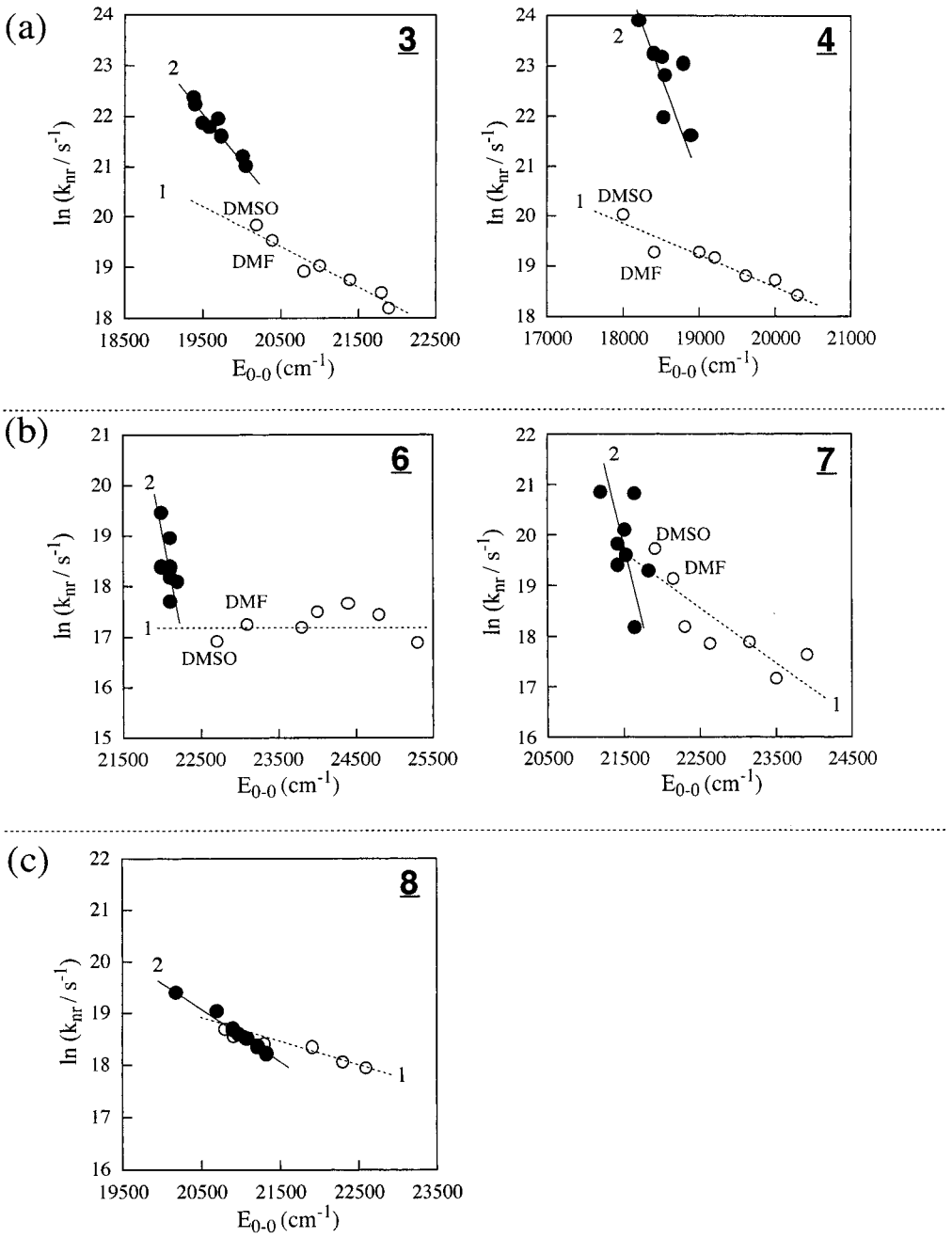

Figure 7. Correlation between the S_1-S_0 energy gap and the logarithm of the nonradiative deactivation rate constants for **3**, **4**, and **6**−**8**: (solid circles) protic solvents (ethanol, methanol, 1-propanol, 2-propanol, 1-butanol, *tert*-butyl alcohol, 1-octanol, and ethylene glycol); and (open circles) aprotic solvents (benzene, diethyl ether, ethyl acetate, butyronitrile, acetonitrile, DMF, and DMSO).

According to HSAB theory, a hard base such as an alkylamine or hydroxide ion has its negative charge localized on a specific atom with high electronegativity, whereas benzene is a typical soft base, in which the electrons are delocalized. The distributions of the negative charge calculated for the excited compounds (**1**−**10**), shown in Table 1 and Figure 9, allow one to classify the excited states for compounds **1**−**7** as "hard anions" in which the negative charge is localized on the carbonyl oxygen and the excited compounds **8**−**10** as "soft anions" in which the negative charge is delocalized. The hydroxyl hydrogen of the quencher alcohol is protic and should be classified as a "hard cation." The hard anions, i.e., the excited states of molecules **1**−**7**, can be well understood to interact on the carbonyl oxygen with the hard cation, i.e., the hydroxyl hydrogen of the quencher alcohol. On the other hand, the soft anions, i.e., the excited states of molecules **8**−**10**, would not have an appreciable interaction with the hard cation, the hydroxyl hydrogen of the alcohol, because of the diffuse distribution of their negative charge. These speculations are well correlated with the experimental result that the fluorescence behavior for compounds **1**−**7** is significantly affected by alcohols, whereas that for compounds **8**−**10** is nearly insensitive to alcohols.

As seen in Figure 9, for compounds **1**−**4**, the negative charge density on the carbonyl oxygen in the excited state is higher or about as high as on the other parts of the molecules. Consequently, a strong hydrogen bond can be formed between the excited molecules and alcohol. However, for compounds **5**−**7**, the negative charge density on the carbon atoms of the aromatic ring is higher than that on the carbonyl oxygen. The dipole−dipole interaction between the aromatic ring and the alcohol also plays an important role (as indicated by the substantial red shift of the fluorescence spectra) and competes with the

TABLE 5: Differences in the Logarithm of the Nonradiative Decay Rate Constant in Alcohol between Experimental Values and Values Expected from the Correlation in Aprotic Solvents

	in ethanol		in methanol	
	$E_{0-0}/10^4$ cm^{-1}	$\Delta\ln(k_{nr}/s^{-1})^a$	$E_{0-0}/10^4$ cm^{-1}	$\Delta\ln(k_{nr}/s^{-1})^a$
1	1.88	1.9	1.88	2.3
2	1.80	2.9	1.78	3.0
3	1.97	1.9	1.94	1.9
4	1.84	3.7	1.82	4.2
5	2.25	0.75	2.25	1.3
6	2.21	1.1	2.21	1.6
7	2.15	0.75	2.16	1.5
8	2.09	−0.22	2.07	0.14
9	2.30	−0.2	2.31	0.14
10	2.20	−0.10	2.18	0.28

[a] Difference in the logarithm of the nonradiative decay rate constant in alcohol between experimental value and value expected from the linear correlation in aprotic solvents using E_{0-0} in alcohol.

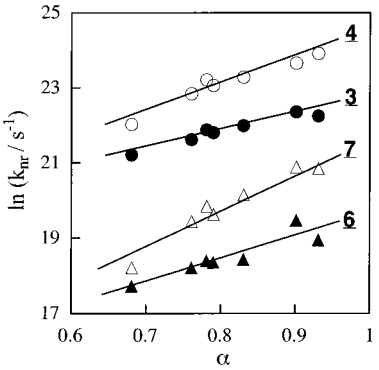

Figure 8. Correlation between the logarithm of the radiationless deactivation rate constant (ln k_{nr}) and the Taft hydrogen-bonding donating parameter (α).

hydrogen bonding interaction between the oxygen atom of the molecule and the alcohol.

Anomalous Behavior of Aminophthalimides: Other Factors Controlling the Radiationless Deactivation. The HSAB rule adopted above should be reasonable for understanding the fluorescence quenching phenomena for compounds **1**−**10**. The fluorescence behavior of compounds **5**−**7**, however, is not fully understood. As indicated above, the excited states of molecules **5**−**7** should be classified as hard anions, in which the negative charge is localized on the carbonyl oxygen (Figure 9). A substantial interaction of ethanol with the excited state of molecules **5**−**7** is certainly induced, as observed by changes in the fluorescence spectrum (Figure 2b). The relaxed state of the hydrogen-bonded species (with a maximum at ca. 450 nm), however, is rather emissive, and radiationless deactivation is not as efficient as that for compounds **1**−**4**. Therefore, factors other than the charge distribution change should control the deactivation in the relaxed hydrogen-bonded state. We have already found that the intermolecular hydrogen bonding in the excited state is anisotropic with respect to the molecular plane; both an emissive in-plane bending mode hydrogen-bonded species and a nonemissive out-of-plane bending mode species exist in the excited state (Figure 10).[14−16] Recently, we have further succeeded in the direct detection of the two species by transient absorption studies.[17] The out-of-plane mode species is presumed to induce an efficient deactivation process through the out-of-plane bending motion of the carbonyl group as an accepting mode for the deactivation. In this case, the degree of bending motion is thought to affect the degree of deactivation.

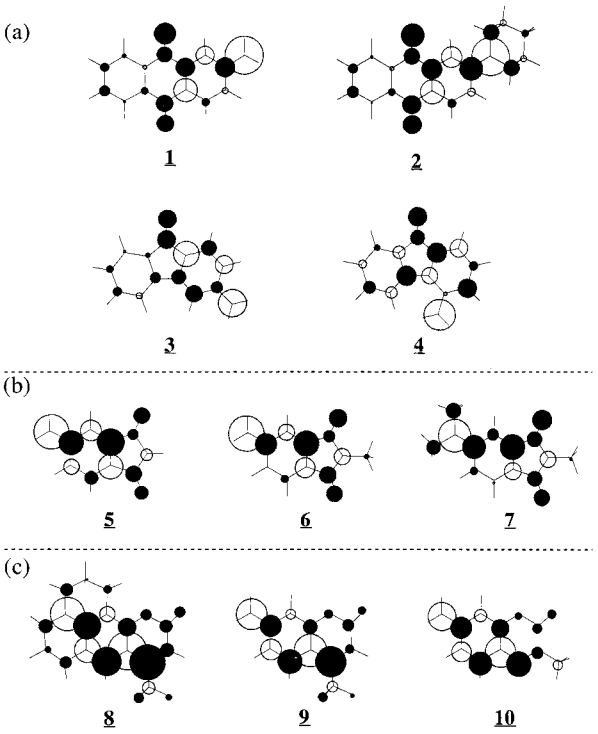

Figure 9. Partial charge changes on particular atoms of molecules **1**−**10** by photoexcitation. The areas of the open and closed circles correspond to the amounts of positive and negative charge, respectively.

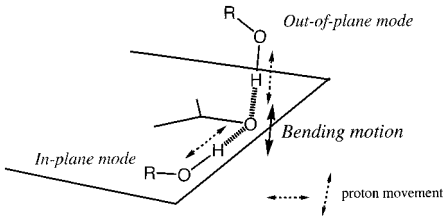

Figure 10. Schematic diagram showing two types of hydrogen bonding modes and the bending motion proposed to promote effective radiationless deactivation.

One of the most promising approaches toward an improved understanding of the different efficiencies of deactivation from the relaxed state between **1**−**4** and **5**−**7** would be a consideration of differences in molecular rigidity for the bending motion. A different degree of rigidity for any of the molecules **5**−**7** might result in an inefficient accepting mode for the deactivation. To clarify these most interesting points, detailed vibrational analyses in the excited state are required and are now in progress.

Conclusions

The photophysical and photochemical properties of the ICT state of aromatic compounds in protic solvents were observed to be very much dependent on the degree of charge separation and charge localization on a specific atom within the excited molecule. The HSAB concept was successfully introduced to explain the different types of quenching behavior by ethanol. The excited molecule was classified as (1) a hard anion when the negative charge is mostly localized on the carbonyl oxygen and (2) a soft anion when the negative charge is not explicitly localized on the carbonyl oxygen but is delocalized over the whole molecule. Among the excited molecules **1**−**7** with the hard anion-type carbonyl oxygen, the excited compounds **1**−**4** underwent significant quenching by intermolecular hydrogen bonding with ethanol, whereas ethanol did interact effectively

but did not induce an efficient deactivation in the relaxed excited molecules **5**−**7**. The deactivation of the other excited molecules **8**−**10** classified as soft anions was not affected by ethanol.

Acknowledgment. This work was partly supported by a Grant-in Aid from the Ministry of Education, Science, Sports, and Culture of Japan.

References and Notes

(1) Maroncelli, M.; Macinnis, J.; Fleming, G. R. *Science* **1989**, *243*, 1674.

(2) Maroncelli, M. *J. Mol. Liq.* **1993**, *57*, 1.

(3) Phelps, D. K.; Weaver, M. J.; Ladanyi, B. M. *Chem. Phys*. **1993**, *176*, 575.

(4) Kumar, P. V.; Maroncelli, M. *J. Chem. Phys.* **1995**, *103* (*8*), 3038.

(5) (a) Kang, T. J.; Ohta, K.; Tominaga, K.; Yoshihara, K. *Chem. Phys. Lett.* **1998**, *287*, 29. Ohta, K.; Kang, T. J.; Tominaga, K.; Yoshihara, K. *Chem. Phys.* **1999**, *242*, 103. (b) Castner, E. W., Jr.; Maroncelli, M.; Fleming, G. R. *J. Phys. Chem*. **1987**, *86*, 1090. Stratt, R. M.; Maroncelli, M. *J. Phys. Chem*. **1996**, *100*, 12981. Horng, M. L.; Gardecki, J. A.; Maroncelli, M. *J. Phys. Chem. A.* **1997**, *101*, 1030. (c) Horng, M. L.; Gardecki, J. A.; Papazyran, A.; Maroncelli, M. *J. Phys. Chem.* **1995**, *99*, 17311.

(6) (a) Gutavsson, T.; Cassara, L.; Gulibinas, V.; Gurzadyan, G.; Mialocq, J.-C.; Pommeret, S.; Sorgius, M.; van der Meulen, P. *J. Phys. Chem. A* **1998**, *102*, 4229. (b) Jarzeba, W.; Walker, G. C.; Johnson, A. E.; Barbara, P. F. *Chem. Phys*. **1991**, *152*, 57. (c) Shirota, H.; Pal, H.; Tominaga, K.; Yoshihara, K. *J. Phys. Chem*. **1996**, *100*, 14575.

(7) Chapman, C. F.; Fee, R. S.; Maroncelli, M. *J. Phys. Chem*. **1995**, *99*, 4811.

(8) Jones, G., II.; Jackson, W. R.; Choi, C.; Bergmark, W. R. *J. Phys. Chem*. **1985**, *89*, 294.

(9) (a) Cichos, F.; Willert, A.; Rempel, U.; von Borczyskowski, C. *J. Phys. Chem. A* **1997**, *101*, 8179. (b) Cichos, F.; Brown, R.; Rempel, U.; von Borczyskowski, C. *J. Phys. Chem. A* **1999**, *103*, 2506.

(10) Werner, T. C.; Hoffman, R. M. *J. Phys. Chem.* **1973**, *77*, 1611. Declemy, A.; Rulliere, C.; Kottis, P. *Chem. Phys. Lett.* **1983**, *101*, 401.

(11) Chudoba, C.; Nibbering, E. T. J.; Elsaesser, T.; *J. Phys. Chem. A.* **1999**, *103*, 5625. Nibbering, E. T. J.; Tschirschwitz, T.; Chudoba, C.; Elsaesser, T.; *J. Phys. Chem. A.* **2000**, *104*, 4236.

(12) Inoue, H.; Hida, M.; Nakashima, N.; Yoshihara, K. *J. Phys. Chem*. **1982**, *86*, 3184.

(13) Yatsuhashi, T.; Nakajima, Y.; Shimada, T.; Inoue, H. *J. Phys. Chem. A* **1998**, *102*, 3018.

(14) Yatsuhashi, T.; Inoue, H. *J. Phys. Chem. A* **1997**, *101*, 8166.

(15) Yatsuhashi, T.; Nakajima, Y.; Shimada, T.; Inoue, H. *J. Phys. Chem. A* **1998**, *102*, 8657.

(16) Sugita, M.; Shimada, T.; Tachibana, H.; Inoue, H. *Phys. Chem. Chem. Phys.* **2001**, *3*, 2012.

(17) Morimoto, A.; Yatsuhashi, T.; Shimada, T.; Kumazaki, S.; Yoshihara, K.; Inoue, H. *J. Phys. Chem. A* **2001**, *105*, 8840.

(18) Le Bris, M. T. *J. Heterocyclic Chem.* **1984**, *21*, 551.

(19) Melhuish, W. H. *J. Phys. Chem.* **1961**, *65*, 229.

(20) Riddick, J. A.; Bunger, W. B.; Sakano, T. K. *Organic Solvents*, 4th ed.; John Wiley & Sons: New York, 1986.

(21) Biczók, L.; Bérces, T.; Márta, F. *J. Phys. Chem.* **1993**, *97*, 8895.

(22) (a) Lippert, E. *Z. Naturforsch*. **1955**, 541; *Z. Elektrochem*. **1957**, *61*, 962. (b) Mataga, N.; Kaifu, Y.; Koizumi, M. *Bull. Chem. Soc. Jpn.* **1955**, *28*, 690; **1956**, *29*, 465.

(23) Fernandez Pacios, L. *ARVOMOL*, version 2; QCPE Program 132, 1994; Department Quimica y Bioquimica ETIS, Montes University Politecnica de Madrid: Madrid, Spain, 1994.

(24) Englman, R.; Jortner, J. *J. Mol. Phys.* **1970**, *18*, 145.

(25) Biczók, L.; Bérces, T.; Inoue, H. *J. Phys. Chem. A* **1999**, *103*, 3837.

(26) Tetreault, N.; Muthyala, R, S.; Liu, R, S, H.; Steer, R P. *J. Phys. Chem. A* **1999**, *103*, 2524.

(27) Biczók, L.; Yatsuhashi, T.; Bérces, T.; Inoue, H. *Phys. Chem. Chem. Phys.* **2001**, *3* (6), 980.

(28) Jones, G., II.; Griffin, S. F.; Choi, C.; Bergmark, W. R. *J. Org. Chem.* **1984**, *49*, 2705.

(29) Kamlet, M. J.; Abboud, J. M.; Abraham, M. H.; Taft, R. W. *J. Org. Chem.* **1996**, *48*, 2877.

(30) Pearson, R. G. Ed.; *Hard and Soft Acids and Bases*; Hutchingson and Ross: Stroudsburg, Pennsylvania, 1973. Ho, T.-l. *The Hard and Soft Acid and Base Principle in Organic Chemistry*; Academic Press: New York, 1977.